Title: HRCT texture analysis for pure or part-solid ground-glass nodules: distinguishability of adenocarcinoma in situ or minimally invasive adenocarcinoma from invasive adenocarcinoma

Authors:

Takuya Yagi[1], Motohiko Yamazaki[1], Riuko Ohashi[2], Rei Ogawa[1], Hiroyuki Ishikawa[1], Norihiko Yoshimura[1], Masanori Tsuchida[3], Yoichi Ajioka[4] , Hidefumi Aoyama[1]

1. Department of Radiology and Radiation Oncology, Niigata University Graduate School of Medical and Dental Sciences, 1-757 Asahimachi-dori, Chuo-ku, Niigata-City, Niigata, 951-8510, Japan.
2. Histopathology Core Facility, Niigata University Faculty of Medicine
3. Division of Thoracic and Cardiovascular surgery, Niigata University Graduate School of Medical and Dental Sciences
4. Division of Molecular and Diagnostic Pathology, Niigata University Graduate School of Medical and Dental Sciences

Corresponding author: Motohiko Yamazaki
Mailing address: Department of Radiology and Radiation Oncology, Niigata University Graduate School of Medical and Dental Sciences, 1-757 Asahimachi-dori, Chuo-ku, Niigata-City, Niigata, 951-8510, Japan.

Tel: +81252272315
Fax: +81252270788
E-mail: xackey2001@gmail.com

The type of manuscript: Original article
The word count: 2539
Conflict of Interest: The authors declare that they have no conflict of interest.

*This work was supported by JSPS KAKENHI Grant Number JP17K10352.

Ethical statement

An institutional review board approved this retrospective study and waived the requirement for informed consent.

Abstract

Purpose: To distinguish between adenocarcinoma in situ (AIS) –minimally invasive adenocarcinoma (MIA) and invasive adenocarcinoma (IAC) showing pure or part-solid ground-glass nodules (GGNs) by high-resolution computed tomography (HRCT) texture analysis.

Materials and methods: This retrospective study included 101 consecutive patients with 115 pure or part-solid GGNs ≤3-cm diameter, which were surgically resected and pathologically diagnosed with AIS, MIA, or IAC (48 AIS–MIA and 67 IAC) between April 2011 and March 2015. Each tumor was manually segmented on axial CT images, and the following texture features were calculated: volume, mass, mean CT value, variance, skewness, kurtosis, entropy, uniformity, and percentile CT numbers (10th, 25th, 50th, 75th, 90th, 95th percentiles). The differences between AIS–MIA and IAC were statistically evaluated using univariate, multivariate, and receiver operating characteristic analysis.

Results: Compared with IAC, AIS-MIA had significantly greater skewness, kurtosis, and uniformity, whereas in the other parameters, AIS-MIA demonstrated significantly lower values than those of IAC. Multivariate

analysis revealed that independent differentiators were the 90th percentile CT numbers ($P < 0.001$) and entropy ($P = 0.005$) with an excellent accuracy (area under the curve, 0.90).

Conclusions: The 90th percentile CT numbers and entropy can accurately distinguish AIS–MIA from IAC.

Key words:

Ground-glass nodule;

Adenocarcinoma in situ;

Minimally invasive adenocarcinoma;

Texture analysis;

High-resolution computed tomography

Introduction

In 2011, the International Association for the Study of Lung Cancer/American Thoracic Society/European Respiratory Society (IASLC/ATS/ERS) proposed a new multidisciplinary classification for lung adenocarcinoma [1], which was issued as the WHO classification 4th edition in 2015 [2]. Based on this classification, lung adenocarcinoma is classified as adenocarcinoma in situ (AIS), minimally invasive adenocarcinoma (MIA), and invasive adenocarcinoma (IAC). If AIS and MIA are completely resected, the 5-year survival rates are 100% and near 100%, respectively [2], whereas the 5-year survival rate of IAC of pathological stage IA is 74.6% [3]. Therefore, it may be clinically significant to distinguish between AIS–MIA and IAC before surgical resection because AIS–MIA with a good prognosis may be suitable candidates for sublobar resection such as segmentectomy and wedge resection [4, 5]. Several studies on the distinction between AIS–MIA and IAC have been reported to date. However, according to previous studies, it is difficult to differentiate between the two groups using only visual CT assessment [6, 7, 8].

Recently, it has become possible to quantitatively evaluate the density of

each voxel in CT images and to analyze texture features of the tumor [9]. The usefulness of texture analysis has been reported in the field of lung cancer [10, 11]; however, few studies have investigated the distinguishability of AIS, MIA, and IAC.

Chae et al. investigated the ability to differentiate between atypical adenomatous hyperplasia (AAH)–AIS and MIA–IAC groups appearing as part-solid GGNs by texture analysis [12]. Although researchers distinguished between AIS and MIA, both groups have a 5-year survival rate of near 100%, and there is no difference in prognosis [1]. Son et al. examined the ability to distinguish AIS–MIA from IAC in GGNs containing no or little solid components with a diameter of <5 mm by texture analysis [13]. However, Fleischner Society recommends that GGNs with a solid component diameter of <6 mm should be followed up without surgery [14].

From the above, when judging candidates of sublobar resection based on the expected prognosis before surgery, it is important to differentiate AIS–MIA from IAC and to investigate GGNs with a solid component diameter of not only ≤5 mm but also >5mm because AIS–MIA and IAC have clearly different prognosis, and GGNs that are generally considered for surgery have a solid

component of >5 mm. However, these considerations have not been examined in the past. In addition, the previous studies did not evaluate tumor texture using high-resolution CT (HRCT), but used conventional thin-slice CT [12, 13]. HRCT provides more detailed texture information because it has higher spatial resolution than that of conventional thin-slice CT. If AIS–MIA and IAC can be accurately distinguished by HRCT texture analysis before surgery, it will help to determine the clinical strategy, such as sublobar surgery or follow-up without surgery.

Therefore, the aim of this study was to examine the distinguishability of AIS–MIA and IAC showing pure or any part-solid GGNs using HRCT texture analysis.

Materials and methods

An institutional review board approved this retrospective study and waived the requirement for informed consent. From April 2011 to March 2015, 220 consecutive patients were pathologically diagnosed with primary lung adenocarcinoma based on the WHO classification 4th edition after surgical resection. We excluded 119 cases due to the following factors: (1) Non-

enhanced CT was not performed at our hospital (n = 14), (2) Tumors > 3-cm diameter (n = 39), (3) Solid nodules without ground-glass opacity (GGO) (n = 62), (4) Unclear margin owing to interstitial pneumonia around the nodule (n = 2), and (5) No nodule detection in CT (n = 2). Finally, 101 patients (45 men and 56 women, mean age ± standard deviation = 69.42 ± 7.8 years; age range, 44–88 years) with 115 nodules showing ≤3 cm of pure GGN or part-solid GGN were included in our study. Eighty-nine patients had a single primary lesion and 12 patients had multiple primary lesions (10 and two patients had two and three nodules, respectively). From the pathologic analysis, 16 were diagnosed as AIS, 32 as MIA, and 67 as IAC. Subtypes of IAC included papillary predominant (n = 46), acinar predominant (n = 1), lepidic predominant (n = 11), micropapillary predominant (n = 2), solid with mucin (n = 3), and invasive mucinous (n = 4). The median interval between CT examination and surgery was 3 days (range, 2–128 days; Table 1).

CT protocol

CT images were obtained using the following four multidetector-row CT scanners: Somatom Definition flash (Siemens, Germany), Aquilion 64

(Toshiba, Japan), Elite Ingenuity (Philips, Nederland), and Aquilion ONE (Toshiba, Japan). Of these, Somatom Definition flash was mainly used. Although some CT examinations were performed with contrast material, only non-contrast enhanced images were used for this study. The scanning parameters for HRCT were as follows: Tube current, automatic exposure control (AEC); Tube voltage, 120 kVp; Detector pitch, 0.8–1.172 mm; Detector collimation, 64–80 × 0.025–0.6 mm; Gantry rotation time, 0.4–0.5 s; Field of view, 200 × 200; Pixel spacing, 512 × 512; and Reconstruction slice thickness, 1 mm. Sharp algorithm was used for all reconstruction factors. Other HRCT scanning parameters for each scanner are summarized in Table 2.

Quantitative analysis

The acquired DICOM data were transferred to a personal computer, and a radiologist with 10 years of experience in chest radiology performed image analysis using ImageJ [15, 16]. First, to reduce the effect of image noise on CT texture parameters, outlier voxels were modified using a median filter, which replaces the pixel value of interest with the median value of the region that is set by the user. The set region in this study was a circle with a radius

of 2 pixels centered on the pixel of interest. Subsequently, each nodule was manually contoured by covering all axial sections in which a nodule appeared (Fig. 1), while normal vessels in the nodules were excluded as much as possible. Consequently, the CT value for each voxel of the whole nodule was extracted. The acquired data were saved, and the following quantitative analysis parameters were then calculated: volume, mass, mean CT value, variance, skewness, kurtosis, entropy, uniformity, and percentile CT numbers (10th, 25th, 50th, 75th, 90th, and 95th percentiles of the CT number). For the calculation of mass, the following equation from a previous study [17] was used:

Mass (mg) = (mean CT values + 1000) × volume (ml)

Detailed information on texture features were defined from a previous report [18] and are described in the Supplementary Appendix.

Pathological evaluation

All 115 surgically resected nodules were diagnosed based on the WHO classification 4th Edition by a pathologist with 16 years of experience in pulmonary pathology. All resected specimens were formalin fixed, paraffin

embedded, hematoxylin eosin stained, and diagnosed. Elastica van Gieson stain was added to specimens that were difficult to determine the diameter of invasive portion.

Interobserver agreement

To calculate the interobserver agreement of each texture parameter, another radiologist with 12 years of experience in chest radiology contoured 70 nodules resected from June 2013 to March 2015. To evaluate the agreement between the two radiologists, Case 2 of intraclass correlation coefficient (ICC) was used, and the ICC value was considered as follows: 0.0–0.20, slight; 0.21–0.40, fair; 0.41–0.60, moderate; 0.61–0.80, substantial; 0.81–1.00, almost perfect agreement [19].

Statistical analysis

Statistical analyses were performed using Dr.SPSS II and R (version 3.0.2). Student's t-test was used to compare the volumetric and texture parameters of AIS–MIA and IAC. In addition, multivariate analysis (logistic regression analysis) was performed for the parameters that were statistically significant

in the univariate analysis to determine independent differentiators between AIS–MIA and IAC using a forward selection method. Receiver operating characteristic (ROC) analyses were conducted for the parameters determined as independent differentiators in the multivariate analysis, and the distinguishability of AIS–MIA and IAC was evaluated using area under the curve (AUC). The Youden index was used to determine the optimal cut-off value. In cases where more than one feature was statistically significant in multivariate analysis, the predicted values of IAC were calculated by combining multiple features using the following equation:

$$\text{Predicted values of IAC} = B0+B1X1+B2X2+\cdots+BpXp$$

where B0 is a constant, B1–Bp are partial regression coefficients, any of which are numerical values determined from logistic regression analysis, and X1–Xp are statistically significant texture features. The AUC was then acquired by comparing the predicted values and the actual pathological results (i.e., AIS–MIA or IAC). P values < 0.05 were considered statistically significant.

Results

Univariate analysis

In the univariate analysis, significant differences in all texture parameters were observed between AIS–MIA and IAC. The values for skewness, kurtosis, and uniformity of AIS-MIA were significantly higher compared to those of IAC. The values of other parameters were significantly lower for AIS-MIA than those for IAC (Table 3).

Multivariate analysis

For the multivariate analysis, we used all parameters that were statistically significant in the univariate analysis: volume, mass, mean CT value, variance, skewness, kurtosis, entropy, uniformity, and 10th, 25th, 50th, 75th, 90th, and 95th percentile CT numbers. It was revealed that 90th percentile CT numbers [adjusted odds ratio (aOR), 1.01; 95% confidence interval (95% CI), 1.006, 1.013; $P < 0.001$) and entropy (aOR, 18.361; 95% CI, 2.422, 139.21; $P = 0.005$) were independent differentiators of AIS–MIA from IAC (Table 4).

ROC analysis

ROC analysis was conducted for the 90th percentile CT numbers and entropy, which were defined as independent differentiators in the multivariate analysis. The optimal cut-off value for the 90th percentile CT numbers was −182.5 HU (specificity, 0.81; sensitivity, 0.84), and the AUC was 0.87 (95% CI, 0.81–0.94). The optimal cut-off value for entropy was 9.33 (specificity, 0.75; sensitivity, 0.85), and the AUC was 0.85 (95% CI, 0.78–0.92). The AUC obtained by combining the two parameters was 0.90 (95% CI, 0.84–0.95), indicating excellent distinguishability (Table 5; Fig. 2A-C; Fig. 3).

Interobserver agreement

The ICC was as follows: volume, 0.85 (95% CI, 0.76–0.93); mass, 0.93 (0.79–0.97); mean CT value, 0.89 (0.17–0.97); variance, 0.81 (0.51–0.91); skewness, 0.89 (0.61–0.96); kurtosis, 0.92 (0.87–0.95); entropy, 0.88 (0.58–0.95); uniformity, 0.80 (0.59–0.89); 10th, 0.65 (−0.036–0.87); 25th, 0.73 (0.040–0.90); 50th, 0.88 (0.24–0.96); 75th, 0.96 (0.71–0.98); 90th, 0.97 (0.91–0.99); and 95th percentile CT numbers, 0.98 (0.95–0.99). The average of all parameters was 0.87. Most parameters were considered to have almost perfect agreement, and the remaining two parameters, namely 10th and 20th percentile CT numbers,

were considered to have substantial agreement.

Discussion

In this study, the 90th percentile CT numbers and entropy were useful to differentiate between AIS–MIA and IAC in lung adenocarcinoma showing pure or part-solid GGNs. The accuracy (AUC = 0.90) was considered to be excellent. While lobectomy is usually selected for IAC due to its poor prognosis, sublobar resection can be applied in the case of AIS–MIA due to its excellent prognosis [4]. Therefore, our results indicate that texture analysis will help determine the suitability of sublobar resection. In addition, because this study used HRCT, the textures of the tumors were evaluated in more detail than those in previous studies that used conventional thin-slice CT.

The 90th percentile CT numbers and entropy were both higher in IAC than those in AIS–MIA. The 90th percentile CT number is a high value among all the voxel densities possessed by the tumor, and our results suggest that this value is strongly associated with a portion of pathological invasion. High entropy indicates the heterogeneity of a tumor. It is well known that a solid portion appears in pure GGO, and its proportion gradually increases as lung

adenocarcinoma progresses from AIS to IAC [20]. We consider that the elevation of entropy reflects the progression of lung adenocarcinoma, namely, the process of changing from pure to heterogeneous GGN due to the mixture of solid portions.

Chae et al. [12] examined the distinguishability between AAH–AIS and MIA–IAC showing part-solid GGNs using CT texture analysis and reported that the AUC was 0.981 by evaluating mean attenuation, standard deviation of attenuation, mass, kurtosis, and entropy. Although the researchers separately assessed AIS and MIA to distinguish between preinvasive and invasive lesions, these two subtypes show similar prognosis (5-year survival rate of 100%). Hence, we believe that it is more important to differentiate AIS–MIA from IAC than to differentiate preinvasive from invasive lesion because AIS–MIA and IAC have clearly different prognosis, and such a difference would affect the selection of sublobar resection candidates.

Son et al. [13] evaluated GGNs with little (≤5 mm) or no solid component by texture analysis and identified that the 75th percentile CT numbers and entropy were the best predictors to distinguish between AIS–MIA and IAC, with an AUC of 0.78. Hwang et al. [21] distinguished preinvasive lesion-MIA

from IAC appearing as pure GGNs and reported that the AUC was 0.962 by combining mass, nodule size, entropy, and homogeneity. While these studies aimed to appropriately diagnose IAC showing GGNs with little solid component to contribute to early intervention (e.g., surgery), the Fleischner Society recommends that GGNs with a solid component diameter of <6 mm should be followed up without surgery [14]. Therefore, we included GGNs with a solid portion diameter of not only ≤ 5 mm but also >5 mm because lobectomy or sublobar resection is generally considered for a solid portion diameter of >5 mm in clinical practice.

Similar to our results, previous studies [13, 21] have reported that entropy is a useful parameter to discriminate between the histologic types of lung adenocarcinoma. High entropy means heterogeneity and is associated with poor prognosis in several tumors, including lung adenocarcinoma [11, 22]. In contrast, although a previous study [13] found that the 75th percentile CT number was a useful parameter, the best predictor of our study was the 90th percentile CT number. This discrepancy may be explained by the fact that our study included GGNs with solid portion diameter of >5 mm, which was excluded from the study population in the previous study; this difference

might have caused the different results.

Previous studies [23, 24] have shown that differences in image quality from the different CT scanners can affect texture features. Mackin et al. [23] evaluated the texture features calculated for 17 CT scanners using a phantom and found the variability in the values of these features. Yosaka et al. [24] investigated how texture features with or without image filtering vary among different CT scanners using a phantom and reported that skewness and kurtosis in filtered images were relatively variable across different CT scanners. Considering these previous studies, the behavior of the texture features of our study among four different CT scanners should be taken into account. Therefore, the reproducibility of our results should be further assessed in a prospective study using identical CT scanners.

Most texture features revealed almost perfect agreement with ICC $\geqq$ 0.80, except for the 10th and 25th percentile CT number. Consequently, texture analysis is considered to be a reproducible method. The reason for the lower ICCs of the 10th and 25th percentile may be the greater influence of these features than that of other higher percentile (i.e., 50th–95th), if normal lung parenchyma was segmented by mistake due to an unclear margin of GGN. To

improve the interobserver agreements, segmentation should be automatically or semi-automatically performed in future analysis.

Our study has several limitations. First, this study was retrospective and performed in a single institution. Second, all nodules were manually contoured; automatic or semi-automatic segmentation was not used. Therefore, small blood vessels that were not excluded may have affected the texture features.

Third, CT images were obtained with four different CT scanners, which may have caused the variability of texture features. Fourth, since image noise of HRCT is commonly high, it may have influenced our results even after application of the median filter. Fifth, second order texture parameters, such as gray-level co-occurrence matrix, were not analyzed. This analysis might improve the distinguishability of AIS–MIA and IAC. Sixth, we did not evaluate the added value of HRCT texture analysis to routine visual assessment.

To conclude, in lung adenocarcinoma showing pure or part-solid GGNs, it is possible to differentiate AIS–MIA, which has a good prognosis, from IAC using the 90th percentile CT numbers and entropy. The results of our study

revealed that HRCT texture analysis can help select candidates for sublobar resection.

References

1. Travis WD, Brambilla E, Noguchi M, et al. International Association for the Study of Lung Cancer/ American Thoracic Society/ European Respiratory Society international multidisciplinary classification of lung adenocarcinoma. J Thorac Oncol 2011; 6(2):244-285
2. Travis, W.D., Brambilla, E., Burke, A.P., Marx, A., Nicholson, A. G. WHO Classification of Tumours of the Lung, Pleura, Thymus and Heart. Fourth edition. 2015
3. Zhang J, Wu J, Tan Q et al. Why do pathological stage IA lung adenocarcinomas vary from prognosis: a clinicopathologic study of 176 patients with pathological stage IA lung adenocarcinoma based on the IASLC/ATS/ERS classification. J Thorac Oncol 2013; 8: 1196-1202
4. Van Schil PE, Asamura H, Rusch VW et al. Surgical implications of the

new IASLC/ATS/ERS adenocarcinoma classification. Eur Respir J. 2012; 39: 478-486

5. Tsutani Y, Miyata Y, Nakayama H et al. Appropriate sublobar resection choice for ground glass opacity-dominant clinical stage IA lung adenocarcinoma wedge resection of segmentectomy. Chest 2014 145:66-71
6. Zhang Y, Shen Y, Qiang JW, et al. HRCT features distinguishing pre-invasive from invasive pulmonary adenocarcinomas appearing as ground-glass nodules. Eur Radiol 2016, 26(9): 2921-8
7. Cohen JG, Reymond E, Lederlin M et al. Differentiating pre- and minimally invasive from invasive adenocarcinoma using CT-features in persistent pulmonary part-solid nodules in Caucasian patients. Eur J Radiol 2015, 84:738-744
8. Lee KH, Goo JM, Park SJ et al. Correlation between the size of the solid component on thin-section CT and the invasive component on pathology in small lung adenocarcinomas manifesting as ground-glass nodules. J Thorac Oncol 2014; 9: 74-82
9. Robert JG, Paul EK, Hedvig H, et al. Radiomics: images are more than pitures, they are data. Radiology 2016; 278: 563-577

10. Kenneth A. Miles. How to use CT texture analysis for prognostication of non-small lung cancer. Cancer Imaging 2016; 16: 10

11. Liu Y, Liu S, Qu F et al. Tumor heterogeneity assessed by texture analysis on contrast-enhanced CT in lung adenocarcinoma: association with pathologic grade. Oncotarget 2017; 8: 53664-53674

12. Chae HD, Park CM, Park SJ, et al. Computerized texture analysis of persistent part-solid ground-glass nodules: differentiation of preinvasive lesions from invasive pulmonary adenocarcinomas. Radiology. 2014; 273: 285-293

13. Son JY, Lee HY, Lee KS, et al. Quantitative CT analysis of pulmonary ground-glass opacity nodules for the distinction of invasive adenocarcinoma from pre-invasive or minimally invasive adenocarcinoma. PLOS ONE. 2014; 9: e104066. doi.org/10.1371/journal.pone.0104066

14. MacMahon H. Naidich DP, Goo JM, et al. Guidelines for management of incidental pulmonary nodules detected on CT images: From the Fleischner Society 2017. Radiology. 2017; 0: 1-16

15. Rasband, W.S., ImageJ, U. S. National Institutes of Health, Bethesda, Maryland, USA, http://imagej.nih.gov/ij/, 1997-2012.

16. Schneider, C.A., Rasband, W.S., Eliceiri, K.W. "NIH Image to ImageJ: 25 years of image analysis". Nature Methods 9, 671-675, 2012.

17. Mull RT. Mass estimates by computed tomography: physical density from CT numbers. AJR 1984, 143:1101-1104

18. Materka A, Strzelecki M. Texture analysis methods-A review. Technical University of Lodz, Institute of Electronics. COST B11 report. 1998

19. Landis JR, Koch GG. The measurement of observer agreement for categorical data. Biometrics 1977, 33:159-174

20. Park CM, Goo JM, Lee HJ et al. Nodular ground-glass opacity at thin-section CT: histologic correlation and evaluation of change at follow-up. Radiographics 27: 391-408

21. Hwang I, Park CM, Park SJ, et al. Persistent pure ground-glass nodules larger than 5 mm: differentiation of invasive pulmonary adenocarcinomas from preinvasive lesions or minimally invasive adenocarcinomas using texure analysis. Invest. Radiol. 2015; 50: 798-804

22. Davnall F, Yip CS, Ljungqvist G et al. Assessment of tumor heterogeneity: an emerging imaging tool for clinical practice? Insights Imaging. 2012; 3:573-589

23. Mackin D, Fave X, Zhang L, et al. Measuring CT scanner variability of radiomics features. Invest Radiol. 2015; 50: 757-765

24. Yasaka K, Akai H, Mackin D, et al. Precision of quantitative computed tomography texture analysis using image filtering: A phantom study for scanner variability. Medicine (Baltimore). 2017; 96(21): e6993. doi: 10.1097/MD.0000000000006993

Table1. Patient characteristic

Characteristic	Number of patients
Men	45
Women	56
Age (y)	69.42 ± 7.8 (44-88)
Pathologic subtype	
AIS	16
MIA	32
IAC	67
Lepidic adenocarcinoma	11
Papillary adenocarcinoma	46
Acinar adenocarcinoma	1
Micropapillary adenocarcinoma	2
Solid adenocarcinoma with mucin	3
Mucinous adenocarcinoma	4

AIS; adenocarcinoma in situ

MIA; minimally invasive adenocarcinoma

IAC; invasive adenocarcinoma

Table 2. HRCT scanning parameters used in the study

	Somatom Difinition Flash	Aquilion 64	Ingenuity Elite	Aquilion ONE
Tube current	AEC	AEC	AEC	AEC
Tube voltage (kVp)	120	120	120	120
Detector pitch (mm)	0.8	0.828	1.172	0.813
Detector collimation (mm)	64 × 0.6	64 × 0.5	64 × 0.025	80 × 0.5
Gantry rotation time (second)	0.5	0.5	0.4	0.5
Field of view (mm)	200 × 200	200 × 200	200 × 200	200 × 200
Pixel spacing	512 × 512	512 × 512	512 × 512	512 × 512
Reconstruction slice thickness (mm)	1	1	1	1
Reconstruction algorism	FBP	FBP	iDose4	AIDR
Reconstruction kernel	B60	FC51	YB	FC51
AEC setting	120ref:mAs CareDose4D	DRI:18 Dose Right index	SD:14 Volume EC	SD:12 Volume EC
mAs (*)	95	75	98	50
CTDIvol (mGy)	6.5	11	6.4	5.7

AEC; auto exposure control

CTDI; CT dose index

FBP; filter back projection

AIDR; adaptive iterative dose reduction

*mAs represents the mean values for Somatom Definition Flash, Ingenuity Elite, and Aquilion ONE and the maximum values for Aqurion 64.

Table 3. Univariate analysis

Characteristic	AIS-MIAs(n=48)	IACs(n=67)	P value
Volume (ml)	2.25 ± 2.45	3.63 ± 2.61	0.005
Mass (mg)	902.3 ± 1002.1	2066.4 ± 1620.3	<0.001
Mean CT value(HU)	-591.3 ± 103.4	-430.5 ± 133.9	<0.001
Variance	36768.2 ± 19078.4	64636.4 ± 17675.4	<0.001
Skewness	0.75 ± 0.57	0.20 ± 0.57	<0.001
Kurtosis	0.55 ± 1.88	-0.68 ± 0.72	<0.001
Entropy	8.97 ± 0.58	9.57 ± 0.23	<0.001
Uniformity	0.0026 ± 0.0013	0.0016 ± 0.00042	<0.001
10^{th} percentile (HU)	-804.7 ± 49.3	-757.1 ± 84.0	0.001
25^{th} percentile (HU)	-733.3 ± 70.6	-639.9 ± 123.5	<0.001
50^{th} percentile (HU)	-624.1 ± 108.7	-448.1 ± 183.5	<0.001
75^{th} percentile (HU)	-481.6 ± 152.2	-234.0 ± 182.6	<0.001
90^{th} percentile (HU)	-335.5 ± 178.7	-88.5 ± 128.6	<0.001
95^{th} percentile (HU)	-248.2 ± 185.4	-31.6 ± 97.1	<0.001

Data are mean ± standard deviation.

HU; hounsfield unit

AIS; adenocarcinoma in situ

MIA; minimally invasive adenocarcinoma

IAC; invasive adenocarcinoma

Table 4. Multivariate analysis

Variables	Odds Ratio	95% CI	P value
90th percentile	1.01	1.006-1.013	<0.001
Entropy	18.361	2.422-139.21	0.005

CI; confidence interval

Table 5. ROC analysis

Predictive factor	Sensitivity	Specificity	AUC(95% CI)
90^{th} percentile + entropy	83.3%	85.1%	0.90 (0.84-0.95)
90^{th} percentile	81.2%	83.6%	0.87 (0.81-0.94)
entropy	75.0%	85.1%	0.85 (0.78-0.92)

The cut-off value of 90th percentile CT numbers is -182.5HU (Hounsfield units)
The cut-off value of entropy is 9.33
ROC; receiver operating characteristics curve
AUC; area under the curve
CI; confidence interval

Figure 1

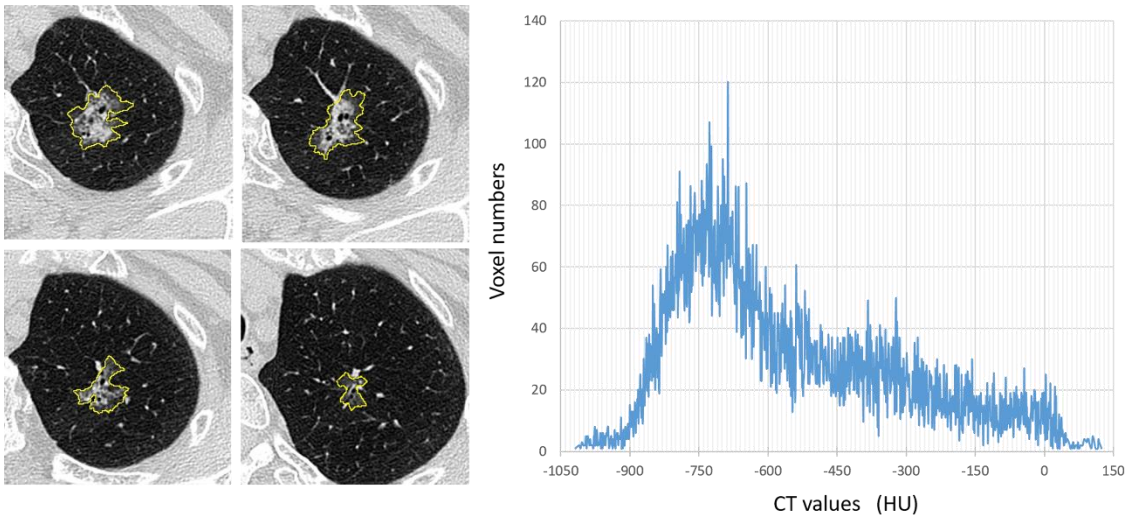

Each tumor was manually segmented at 1 mm intervals on axial CT images and three-dimensionally assessed using the texture analysis software ImageJ.

Figure 2A

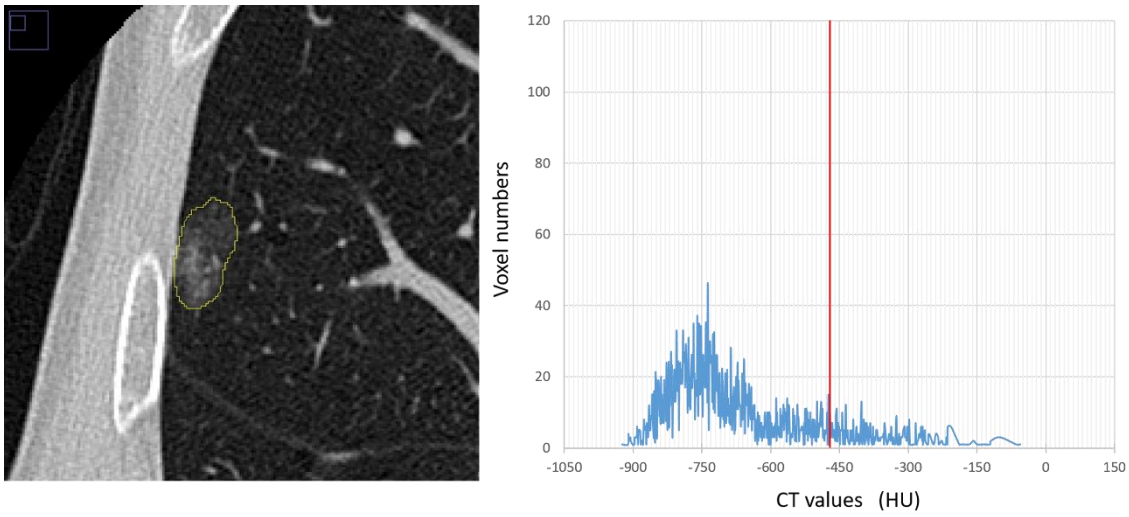

A 70-year-old man with adenocarcinoma in situ (AIS) in the right middle lobe of the lung. In the histogram distribution, the 90th percentile CT number (vertical line) for the case was −471 Hounsfield units (HU), which was lower than the cut-off CT number (−182.5 HU) in this study. The entropy value for the case was 8.69, which was lower than the cut-off value (9.33) in this study.

Figure 2B

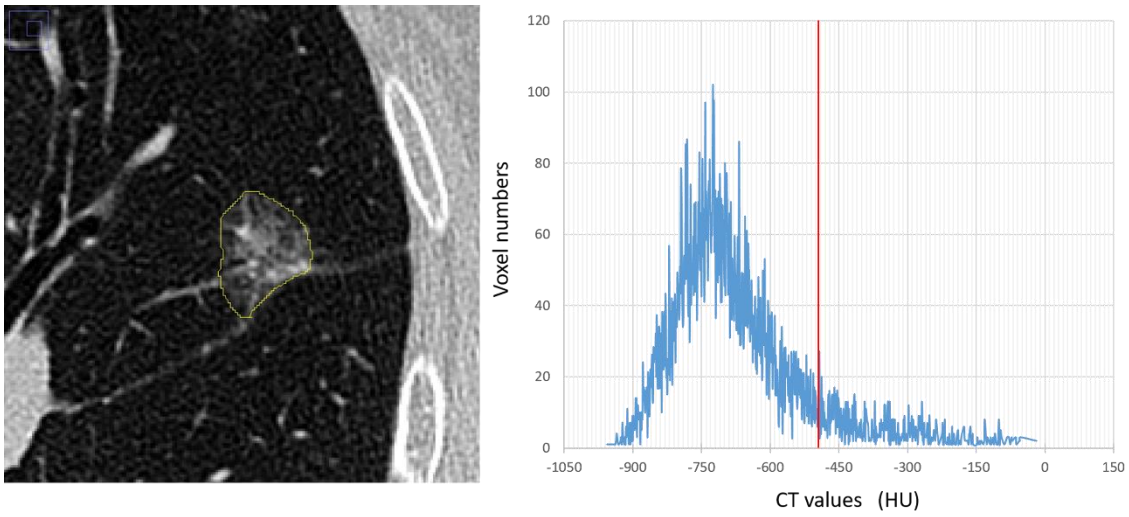

A 77-year-old woman with minimally invasive adenocarcinoma (MIA) in the left upper lobe of the lung. In the histogram distribution, the 90th percentile CT value (vertical line) for the case was −494 Hounsfield units (HU), which was lower than the cut-off CT value (−182.5 HU) in this study. The entropy value for the case was 8.88, which was lower than the cut-off value (9.33) in this study.

Figure 2C

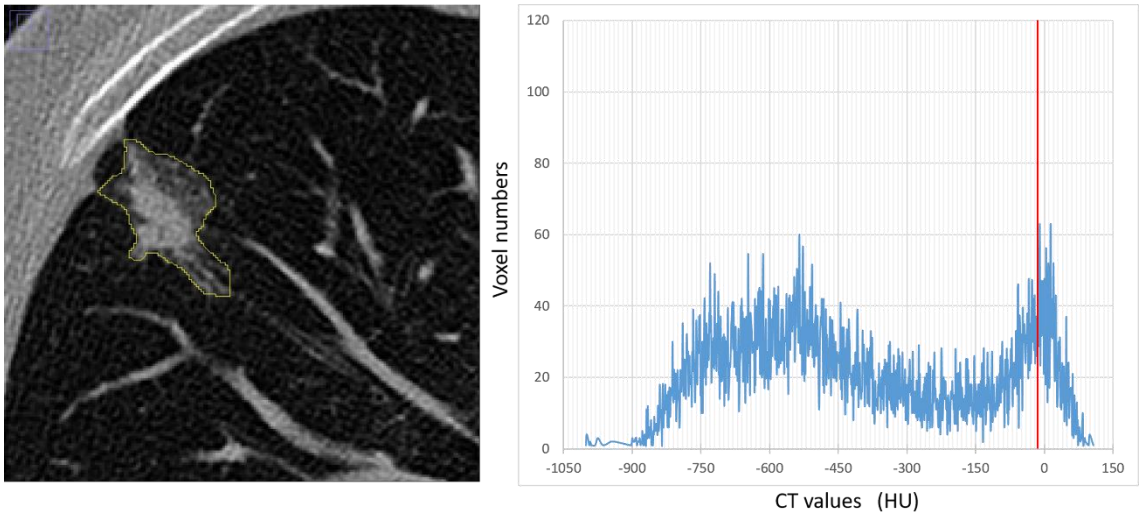

A 69-year-old man with lepidic adenocarcinoma (lepidic IAC) in the right upper lobe of the lung. In the histogram distribution, the 90th percentile CT value (vertical line) for the case was -13 Hounsfield units (HU), which was higher than the cut-off CT value (−182.5 HU) in this study. The entropy value for the case was 9.73, which was higher than the cut-off value (9.33) in this study.

Figure 3

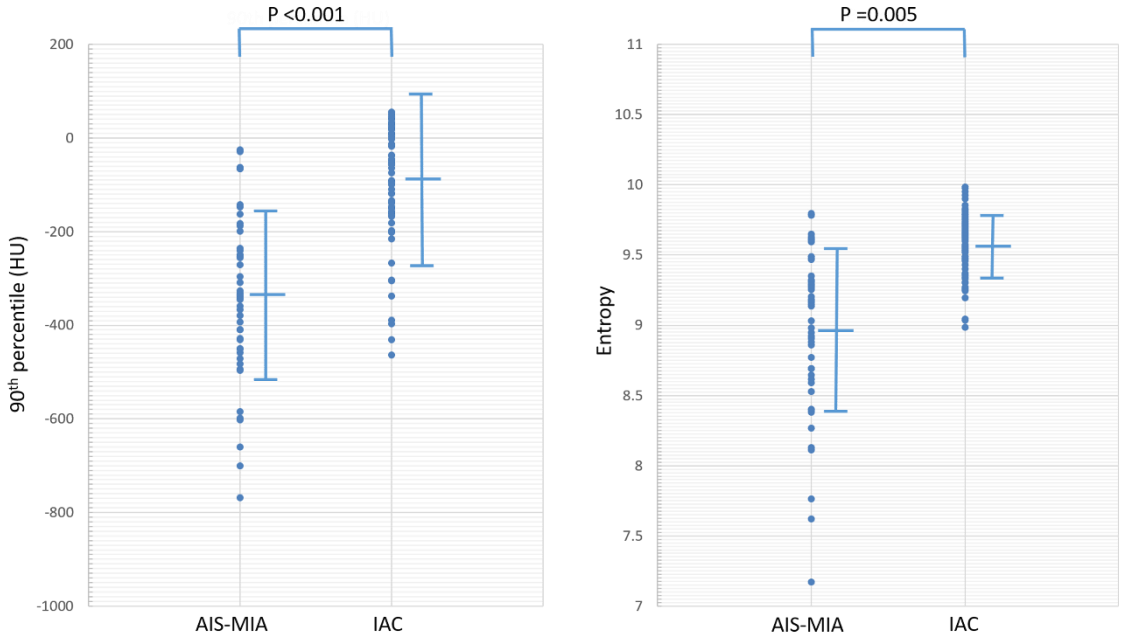

Graphs show 90th percentile CT numbers and entropy of each nodule of 2 groups.

The values for 90th percentile CT numbers of IAC (-88.5 ± 128.6 [mean ± SD]) are higher than those of AIS-MIA (-335.5 ± 178.7). The values for entropy of IAC (9.57 ± 0.23) are higher than those of AIS-MIA (8.97 ± 0.58).

Appendix

i; CT value of a voxel.
$p(i)$; relative frequency of a voxel density.

Mean CT value (μ): The average CT value of the tumor

$$\mu = \sum_{i=0}^{G-1} ip(i)$$

Variance (σ^2): The variation of CT value around the mean

$$\sigma^2 = \sum_{i=0}^{G-1} (i-\mu)^2 p(i)$$

Skewness (μ_3) : A measure indicating the degree of asymmetry of a distribution

$$\mu_3 = \sigma^{-3} \sum_{i=0}^{G-1} (i-\mu)^3 p(i)$$

Kurtosis (μ_4): A measure indicating the degree of sharpness of a histogram peak

$$\mu_4 = \sigma^{-4} \sum_{i=0}^{G-1} (i-\mu)^4 p(i) - 3$$

Entropy (H) and Uniformity (E) : A measure indicating the heterogeneity of a histogram distribution. High entropy and low uniformity mean heterogeneous tumors.

$$\mathrm{H} = -\sum_{i=0}^{G-1} p(i) log_2[p(i)]$$

$$\mathrm{E} = \sum_{i=0}^{G-1} [p(i)]^2$$